Nearly Diffraction-Free Nonlinear Imaging of Irregularly Distributed Ferroelectric Domains

Rong-Er Lu,[1,2] Rui-zhi Zhao,[1,2] Xia Feng,[1,2] Bo Yang,[1,2] Xu-Hao Hong,[1,3] Chao Zhang,[1,2,*] Yi-Qiang Qin,[1,2,†] and Yong-Yuan Zhu[1,3]

[1]*National Laboratory of Solid State Microstructures and Collaborative Innovation Center of Advanced Microstructures and Key Laboratory of Modern Acoustics, Nanjing University, Nanjing 210093, China*

[2]*College of Engineering and Applied Sciences, Nanjing University, Nanjing 210093, China*

[3]*School of Physics, Nanjing University, Nanjing 210093, China*

(Received 14 April 2017; published 8 February 2018)

Second-harmonic generation is used experimentally for the nonlinear imaging of two-dimensional irregular domain structures. Analytical solutions and simulation results for the Fresnel distribution of domain walls are obtained. The results show that the domain wall plays an important role in the imaging process and the corresponding diffraction effect is greatly suppressed (we call it a nearly diffraction-free effect), thus providing a simple way to realize high-resolution imaging for ferroelectric domains.

DOI: 10.1103/PhysRevLett.120.067601

Ferroelectric materials have widespread applications in many different research areas owing to their exotic properties in piezoelectric, pyroelectric, and electro-optical characteristics [1–3]. Because of the emergence of domain wall engineering [4], the study on domain walls in ferroelectric materials has become a hot topic [5–8]. To deeply explore the relationship of the microscopic structures and macroscopic functions, a lot of technologies including electronic microscope and linear optical imaging have been developed to observe domain structures [9–14]. The electronic microscope methods mainly contain scanning electron microscopy (SEM) and transmission electron microscopy (TEM). SEM and its extended techniques have been the most widely used methods at present [15–18], where the contrast between antiparallel ferroelectric domains can be imaged in the secondary electron emission mode. TEM is capable of imaging domain structures directly, and the domain walls in ferroelectric materials such as $LiNbO_3$ can be observed with high resolution [19].

The linear optical imaging for domain observation covers a broader range, including several kinds of microscopic methods [20–25], such as optical microscopy, polarization microscopy, and microwave microscopy. Generally, it is difficult to directly observe domain structures in linear optical methods due to the same refractive index of the antiparallel domains. Thus destructive etching is commonly adopted to change the relevant properties around domain walls for optical observation [26]. In recent years, some nonlinear optical methods, especially second-harmonic generation (SHG) based imaging have emerged. For example, SHG microscopes have been developed to observe the domain structure (or domain wall) nondestructively [27] with a reference SH wave by an interference effect (or without a reference SH wave in a noninterference case) [28]. With the help of the confocal scanning technique, the SHG microscope is able to examine the inner twin boundaries and three-dimensional images for the inner structure can be obtained [29]. A SHG enhancement effect is found in some configurations of SHG and can be exploited to observe the domain wall structure as well [30], and in this situation the domain wall is shown as a bright line in the SH image. Nonlinear Talbot self-imaging is another interesting method for domain characterization [31–34], where periodic domain structures are required and duplicate images of the domain structure are established at specific planes. Besides the Talbot effect, the nonlinear Cherenkov effect can be exploited to observe domain structures as well. With this method, images with high resolution can be obtained by focusing a laser light onto the domain wall and scanning the position of the focus [35].

In this Letter, a simple nonlinear method is introduced for the direct and instant observation of two-dimensional (2D) ferroelectric domain structures in a nonlinear photonic crystal (NPC). The periodicity of domain structure is unnecessary and the focus scanning is also not required, which differs from the Talbot self-imaging method and the nonlinear Cherenkov method. The analytical solution for the nonlinear Fresnel diffraction distribution of domain walls has been deduced theoretically. The result indicates that the SH image of domain walls can be always observed as a dark curve no matter how narrow its width is, and a nearly diffraction-free effect is observed at the same time. The line width of the domain wall image is found to be proportional to the square root of propagation distance, which increases very slowly compared with normal far-field diffraction processes. When moving the object plane away from the crystal surface, the domain wall structure can still be clearly observed within a certain range, which is

quite different from the previous reported SHG imaging approaches, thus providing a possibility for the imaging of sub-wavelength objects with high resolution.

To demonstrate our method of nonlinear SH imaging, we focus on the near-field evolution in the 2D nonlinear propagating process. The NPC fabricated on the z-cut congruent $LiTaO_3$ (CLT) is chosen to be the crystal material with the fundamental wave (FW) at a wavelength of 900 nm propagating along the spontaneous polarization direction. The output SH field can be described by Fresnel diffraction, so the field distribution at the imaging plane can be expressed as

$$E(\alpha,\beta,z)=\frac{e^{ikz}}{i\lambda z}\iint f(x,y)e^{(ik/2z)[(x-\alpha)^2+(y-\beta)^2]}dxdy, \quad (1)$$

where x, y and α, β are the coordinates at the crystal's plane and the imaging plane, respectively. z is the propagating distance, $f(x,y)$ is the NPC structure function, λ is the wavelength of the second-harmonic wave (SHW), and k is the corresponding wave vector.

For an irregularly distributed domain structure, the structure function of the NPC is binary modulated. It means that the function has only two values: $+1$ and -1 because only 180° antiparallel ferroelectric domains exist in our material. First, we have analyzed a simple case that consists of a single domain wall, the corresponding structure function can be written as

$$f(x,y)=\begin{cases}1 & (0<x\le\frac{l}{2},-\frac{h}{2}\le y\le\frac{h}{2})\\ -1 & (-\frac{l}{2}\le x<0,-\frac{h}{2}\le y\le\frac{h}{2})\end{cases}. \quad (2)$$

Here, l and h are the corresponding length and width of the sample unit, respectively. Substituting Eq. (2) into the Fresnel diffraction equation, Eq. (1) can be further simplified [36] so that the light field at the imaging plane can be solved as

$$I(\alpha,\beta,z)=\frac{k^2}{4z^2\pi^2}[H_1(\alpha)+H_2(\alpha)][M_1(\beta)+M_2(\beta)], \quad (3)$$

where

$$\begin{aligned}H_1(\alpha)&=\left(\int_{-\frac{l}{2}}^{0}\cos\frac{k(\alpha+\zeta)^2}{2z}d\zeta-\int_{0}^{l/2}\cos\frac{k(\alpha+\zeta)^2}{2z}d\zeta\right)^2,\\ H_2(\alpha)&=\left(\int_{-(l/2)}^{0}\sin\frac{k(\alpha+\zeta)^2}{2z}d\zeta-\int_{0}^{l/2}\sin\frac{k(\alpha+\zeta)^2}{2z}d\zeta\right)^2,\\ M_1(\beta)&=\left(\int_{-\frac{h}{2}}^{\frac{h}{2}}\cos\frac{k(\beta+\zeta)^2}{2z}d\zeta\right)^2,\\ M_2(\beta)&=\left(\int_{-(h/2)}^{h/2}\sin\frac{k(\beta+\zeta)^2}{2z}d\zeta\right)^2. \quad (4)\end{aligned}$$

The positive domain and the negative domain have the same contribution to the near-field imaging distribution in the aspect of intensity but the phase differs by π. Fresnel diffraction process for the single pair of antiparallel ferroelectric domains is conducted to analyze the nonlinear imaging process. From the simulation of the SH field at a specific plane, as is shown in Figs. 1(a) and 1(b), it can be found that the intensity distribution of the positive domain is the same with the negative domain. Not only for the straight type domain wall, but also for the curving type, the images of domains are bright while the regions of the domain wall are dark. So the clear contrast between domain and domain wall has been established. According to the numerical calculations, we found that the linewidth of the domain wall image can be expressed as a simple expression:

$$w\propto\sqrt{\lambda z}, \quad (5)$$

where w represents the line width of the domain wall image. Interestingly, the domain wall width itself does not appear in the expression, which implies that the domain wall can be always observed in the imaging process no matter how narrow its width is, thus providing a possibility for the imaging of subwavelength objects with high resolution. Figure 1(c) is the simulation result that demonstrates that the line width of the domain wall image is proportional to the

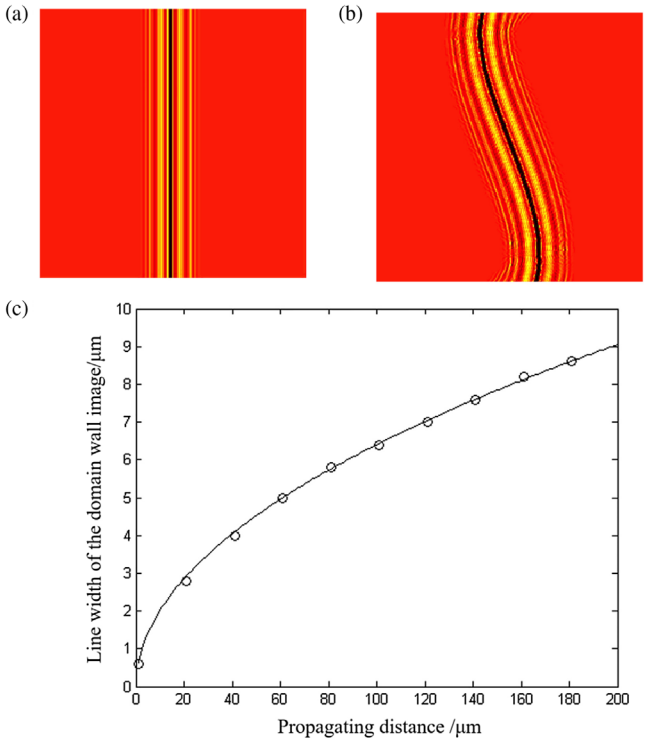

FIG. 1. Simulations of the SH-imaging process for the single antiparallel ferroelectric domain. (a) and (b) The simulated SH-imaging field distributions for the straight and curving wall; (c) the variation of the line width of the domain wall image along with the propagating distance when the wavelength is 450 nm. A power function of the form $w=0.64\sqrt{z}$ (shown as the dark curve) will fit the data points.

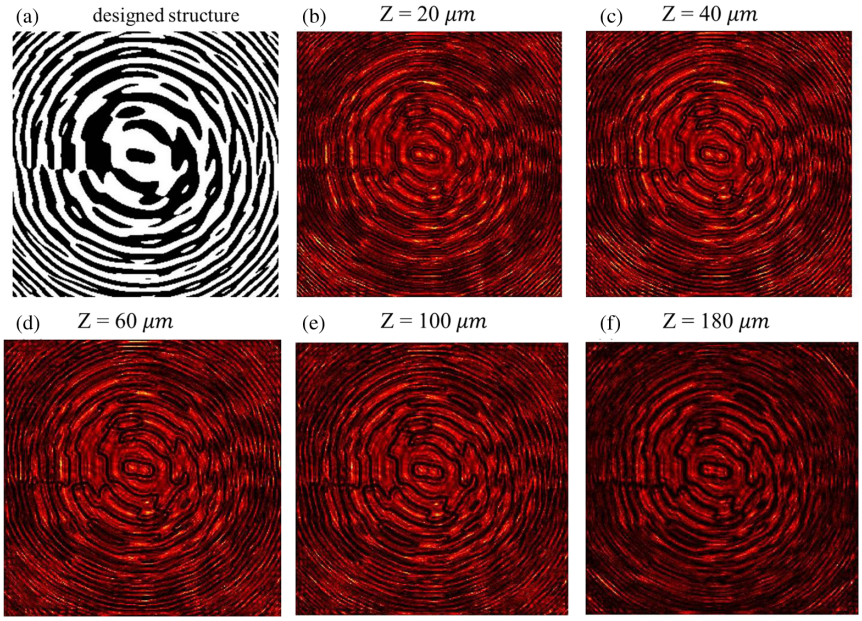

FIG. 2. Simulations of the nonlinear SH imaging processes. (a) The pattern of the designed domain structure. (b)–(f) The SH images at the distance of 20, 40, 60, 100, and 180 μm away from the crystal plane.

square root of the propagation distance with a fixed wavelength. The diffraction effect in this process is greatly suppressed.

Actually, observation of complicated domain structures is more practical in the imaging research area. Inspired by the imaging results of a single domain wall, nonlinear SH imaging for irregularly distributed ferroelectric domain structures has been further investigated. Different from the experimental results in Ref. [30], the SH image of the domain wall exhibits a dark curve with a nearly diffraction-free behavior.

Numerical simulations have been implemented about the nearly diffraction-free propagation process in the near-field region. Figure 2(a) shows the designed domain structure and Figs. 2(b)–2(f) demonstrate the field distributions at different distances away from the crystal plane. The corresponding distances are 20, 40, 60, 100, and 180 μm. The simulation results exhibit that the SHW propagates following certain rules so that the domain structure image is reproduced and kept well within the above-mentioned distance range. That means almost no diffraction effect has emerged. More specifically, although the domain walls have some differences in the thickness of the lines, the whole configuration for the structure matches well with the original designed structure.

We have performed experiments to verify the nearly diffraction-free SH imaging process for irregularly distributed domain structures. The experimental setup is shown in Fig. 3. A femtosecond mode-locked Ti:sapphire laser operating at a wavelength of 900 nm is chosen as the FW source. The NPC structure was fabricated by 2D poling of a 500 μm thick z-cut CLT. The poled area is 500 μm $\times$ 500 μm. A long-pass filter is placed before the sample to filter the visible noise, and a short-pass filter is placed between the sample and the objective lens to eliminate the remaining FW. Unlike the focused fundamental beam used in Refs. [27–29], the laser beam is shaped to be an almost parallel beam propagating along the z axis. Here for the interacting waves propagating along the spontaneous polarization direction of CLT the nonlinear process is oo-o type. Only the d_{21} component contributes to the SHG process in our experimental configuration. The SHW image is recorded by a CCD camera, which is controlled by a precision translation stage so that it can be flexibly moved along the z direction.

There are only two kinds of different domains for $LiTaO_3$ so that the whole domain structure can be seen

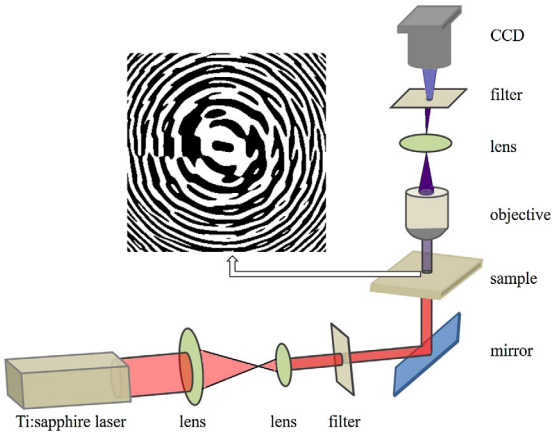

FIG. 3. Schematic of the experimental setup. The laser beam is shaped to be an almost parallel beam propagating along the z axis. The SHG process is carried out and the SHW patterns are recorded at different distances with a CCD camera controlled by a precision translation stage.

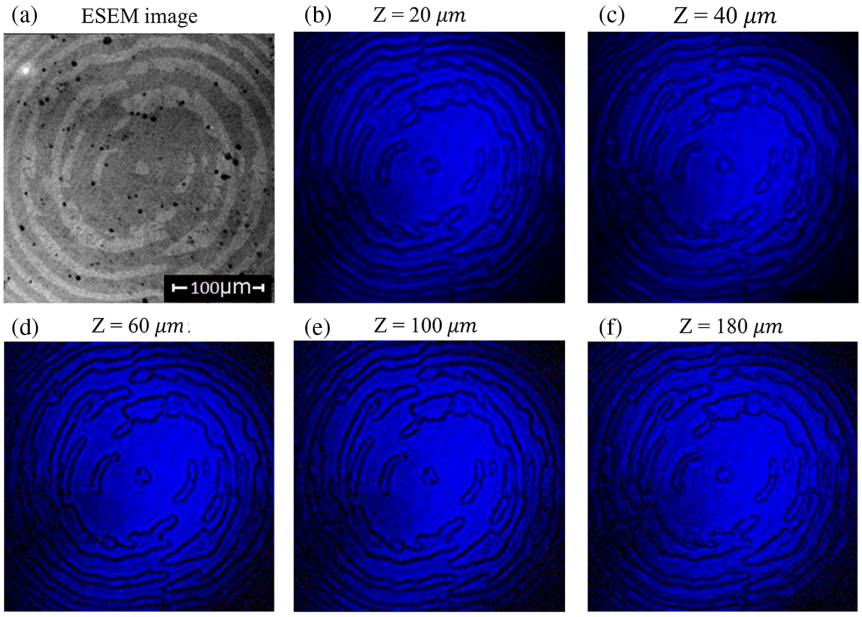

FIG. 4. Contrast images of the domain structures have been established experimentally by the ESEM method (a) and the SH imaging technique (b)–(f); meanwhile, comparisons among different imaging distances of 20, 40, 60, 100, and 180 μm for the SH imaging technique have also been exhibited.

as a combination of many single antiparallel ferroelectric domains. Figure 4 shows the experimental comparison results between the environmental scanning electron microscope (ESEM) and the SH-imaging technique. Figure 4(a) is the domain images obtained by the ESEM, with the image conditions being voltage 30 kV, pressure 30 Pa, spots 5, scan rate 30 μs/frame. The dark spots on the surface may be the destructions to the sample brought by the femtosecond laser in the optical experiment. Figures 4(b)–4(f) are domain patterns detected by the CCD camera at different distances via the SH imaging technique. It can be seen here the domain walls exhibit as dark curves in the SH image. Moreover, we found that when moving the object plane away from the crystal surface, the structure can still be imaged within a range of about 200 μm, which matches well with the simulation results above.

The SH imaging technique has its unique advantages compared with other related methods. Compared with those electron microscopic methods, the direct observation of domain walls instead of antiparallel domains in the SH-imaging process has provided the possibility to the study of domain wall engineering. The preparation steps in linear optical methods such as etching and surface coating are not needed in the SH imaging technique, thus the destruction to samples can be avoided. Furthermore, this method is capable of detecting the domain wall directly and the related diffraction effect is very weak, thus high spatial resolution can be achieved.

In conclusion, the domain wall structures of 2D nonlinear photonic crystals are observed with a simple SH imaging method. Arbitrary ferroelectric domain structures without any periodicity can be observed directly and instantly with this method. The theoretical analysis as well as simulation reveals that the domain wall structure can be always observed in the SH imaging process even when its width is much smaller than the wavelength, and a nearly diffraction-free effect is found at the same time. Compared with the other methods for domain observation, the SH imaging technique has unique advantages such as simplicity, stability, and high imaging resolution, which will lead to many novel discoveries in nonlinear imaging techniques, domain wall engineering, biological detection, and other diverse applications.

This work is supported by the National Key R&D Program of China (2017YFA0303700), the National Natural Science Foundation of China (Grants No. 11774165, No. 11574146, No. 11374150, and No. 11504166), the Jiangsu Science Foundation (BK20150563), and the Priority Academic Program Development of Jiangsu Higher Education Institutions of China (PAPD). We also thank Dr. Dongmei Liu and Dr. Dunzhao Wei for the useful help in the experiments.

*Corresponding author.
zhch@nju.edu.cn
†Corresponding author.
yqqin@nju.edu.cn

[1] I. A. Lukyanchuk, L. Lahoche, and A. Sene, Phys. Rev. Lett. **102**, 147601 (2009).
[2] A. K. Tagantsev, V. O. Sherman, K. F. Astafiev, J. Venkatesh, and N. Setter, J. Electroceram. **11**, 5 (2003).
[3] J. F. Scott and C. A. Paz, Science **246**, 1400 (1989).
[4] E. K. H. Salje, Chem. Phys. Chem. **11**, 940 (2010).

[5] R. K. Vasudevan, A. N. Morozovska, E. A. Eliseev, J. Britson, J. C. Yang, Y. H. Chu, P. Maksymovych, L. Q. Chen, V. Nagarajan, and S. V. Kalinin, Nano Lett. **12**, 5524 (2012).
[6] J. F. Scott, E. K. H. Salje, and M. A. Carpenter, Phys. Rev. Lett. **109**, 187601 (2012).
[7] D. Meier, J. Seidel, A. Cano, K. Delaney, Y. Kumagai, M. Mostovoy, N. A. Spaldin, R. Ramesh, and M. Fiebig, Nat. Mater. **11**, 284 (2012).
[8] E. A. Eliseev, A. N. Morozovska, G. S. Svechnikov, P. Maksymovych, and S. V. Kalinin, Phys. Rev. B **85**, 045312 (2012).
[9] M. Schröder, A. Haußmann, A. Thiessen, E. Soergel, T. Woike, and L. M. Eng, Adv. Funct. Mater. **22**, 3936 (2012).
[10] B. J. Rodriguez, S. Jesse, A. P. Baddorf, and S. V. Kalinin, Phys. Rev. Lett. **96**, 237602 (2006).
[11] E. Soergel, Appl. Phys. B **81**, 729 (2005).
[12] W. Clegg, D. F. L. Jenkins, N. Helian, J. F. C. Windmill, N. Fry, R. Atkinson, W. R. Hendren, and C. D. Wright, IEEE Trans. Instrum. Meas. **51**, 10 (2002).
[13] T. J. Yang, V. Gopalan, P. J. Swart, and U. Mohideen, Phys. Rev. Lett. **82**, 4106 (1999).
[14] J. Kobayashi, Phys. Status Solidi **21**, 151 (1967).
[15] J. F. Ihlefeld, J. R. Michael, B. B. McKenzie, D. A. Scrymgeour, J. P. Maria, E. A. Paisley, and A. R. Kitahara, J. Mater. Sci. **52**, 1071 (2017).
[16] M. Klaui, H. Ehrke, U. Rudiger, T. Kasama, R. E. Dunin-Borkowski, D. Backes, L. J. Heyderman, C. A. F. Vaz, J. A. C. Bland, and G. Faini, Appl. Phys. Lett. **87**, 102509 (2005).
[17] S. Zhu and W. Cao, Phys. Rev. Lett. **79**, 2558 (1997).
[18] R. L. Bihan, Ferroelectrics **97**, 19 (1989).
[19] J. Gonnissen, D. Batuk, G. F. Nataf, L. Jones, A. M. Abakumov, S. Van Aert, D. Schryvers, and E. K. H. Salje, Adv. Funct. Mater. **26**, 7599 (2016).
[20] S. Jesse, B. J. Rodriguez, S. Choudhury, A. P. Baddorf, I. Vrejoiu, D. Hesse, M. Alexe, E. A. Eliseev, A. N. Morozovska, and J. Zhang, Nat. Mater. **7**, 209 (2008).
[21] M. Molotskii, A. Agronin, P. Urenski, M. Shvebelman, G. Rosenman, and Y. Rosenwaks, Phys. Rev. Lett. **90**, 107601 (2003).
[22] T. J. Yang, U. Mohideen, and M. C. Gupta, Appl. Phys. Lett. **71**, 1960 (1997).
[23] H. Luo, Z. Qi, B. Zhang, and W. Zhong, J. Inorg. Mater. **12**, 309 (1997).
[24] F. Saurenbach and B. D. Terris, Appl. Phys. Lett. **56**, 1703 (1990).
[25] Y. Lu, T. Wei, F. Duewer, Y. Lu, N. Ming, P. G. Schultz, and X. D. Xiang, Science **276**, 2004 (1997).
[26] A. Sawada and R. Abe, Jpn. J. Appl. Phys. **6**, 699 (1967).
[27] S. Kurimura and Y. Uesu, J. Appl. Phys. **81**, 369 (1997).
[28] S. I. Bozhevolnyi, J. M. Hvam, K. Pedersen, F. Laurell, H. Karlsson, T. Skettrup, and M. Belmonte, Appl. Phys. Lett. **73**, 1814 (1998).
[29] H. Yokota, H. Usami, R. Haumont, P. Hicher, J. Kaneshiro, E. K. H. Salje, and Y. Uesu, Phys. Rev. B **89**, 144109 (2014).
[30] J. Kaneshiro, Y. Uesu, and T. Fukui, J. Opt. Soc. Am. B **27**, 888 (2010).
[31] J. Wen, Y. Zhang, and M. Xiao, Adv. Opt. Photonics **5**, 83 (2013).
[32] Y. Zhang, J. Wen, S. N. Zhu, and M. Xiao, Phys. Rev. Lett. **104**, 183901 (2010).
[33] H. Jin, P. Xu, J. S. Zhao, H. Y. Leng, M. L. Zhong, and S. N. Zhu, Appl. Phys. Lett. **101**, 211115 (2012).
[34] X. Zhao, Y. Zheng, H. Ren, N. An, and X. Chen, Opt. Lett. **39**, 5885 (2014).
[35] Y. Sheng, A. Best, H. J. Butt, W. Krolikowski, A. Arie, and K. Koynov, Opt. Express **18**, 16539 (2010).
[36] A. Milton, A. S. Irene, and H. R. Robert, *Handbook of Mathematical Functions with Formulas, Graphs, and Mathematical Tables* (U.S. Government Printing Office, Washington, DC, 1964).